

Quantitative evaluation of the damage to RC buildings caused by the 2023 southeast Turkey earthquake sequence

Earthquake Spectra

2024, Vol. 40(1) 505–530

© The Author(s) 2024






Article reuse guidelines:

sagepub.com/journals-permissions

DOI: 10.1177/87552930231211208

journals.sagepub.com/home/eqs

Santiago Pujol, M.EERI¹ , Idris Bedirhanoglu²,
Cemalettin Donmez³, Jeffrey D Dowgala⁴,
Meltem Eryilmaz-Yildirim⁵ , Kari Klaboe, M.EERI⁴,
Fahri Baran Koroglu⁶, Rémy D Lequesne⁷,
Baki Ozturk, M.EERI⁸ , Liam Pledger¹, and
Egemen Sonmez, M.EERI⁹

Abstract

Data from 15 earthquakes that occurred in 12 different countries are presented showing that, without better drift control, structures built with building codes allowing large seismic drifts are likely to keep leaving a wide wake of damage ranging from cracked partitions to building overturning. Following the earthquake sequence affecting south-east Turkey in 2023, a team led by Committee 133 of the American Concrete Institute surveyed nearly 250 reinforced concrete buildings in the area extending from Antakya to Malatya. Buildings ranging from 2 to 16 stories were surveyed to assess their damage and evaluate the robustness of their structures in relation to overall stiffness, as measured by the relative cross-sectional areas of structural walls and columns. The majority of the buildings were estimated to have been built in the past 10 years. Yet, the structures surveyed were observed to have amounts of structural walls and columns comparable with amounts reported after the Erzincan (1992), Duzce (1999), and Bingol (2003) Earthquakes in Turkey. These amounts are, on average, much smaller than the wall and column amounts used in Chile and Japan. Because of that lack of robustness

¹Department of Civil Engineering, University of Canterbury, Christchurch, New Zealand

²Department of Civil Engineering, Dicle University, Diyarbakir, Turkey

³Department of Civil Engineering, Izmir Institute of Technology, Izmir, Turkey

⁴Wiss, Janney, Elstner Associates, Inc., Emeryville, CA, USA

⁵Department of Civil Engineering, Eskisehir Osmangazi University, Eskisehir, Turkey

⁶Department of Civil Engineering, Harran University, Sanliurfa, Turkey

⁷Department of Civil, Environmental, and Architectural Engineering, The University of Kansas, Lawrence, USA

⁸Department of Civil Engineering, Hacettepe University, Ankara, Turkey

⁹Department of Civil Engineering, Izmir University of Economics, Izmir, Turkey

Idris Bedirhanoglu is also affiliated to Department of Engineering Science, Mansfield College, University of Oxford, Oxford, United Kingdom.

Corresponding author:

Meltem Eryilmaz-Yildirim, Department of Civil Engineering, Eskisehir Osmangazi University, Eskisehir 26480, Turkey.
Email: meryilmaz@ogu.edu.tr

and given the intensities of the motions reported from Antakya to Malatya (with 10 stations with peak ground velocity (PGV) of 100 cm/s or more), it is concluded that structures in this region experienced large drifts. Excessive drift (1) exposed a myriad of construction and detailing problems leading to severe structural damage and collapse, (2) induced overturning caused by p-delta for some buildings, and (3) caused widespread damage to brittle masonry partitions. The main lesson is simple: ductility is necessary but not sufficient. It is urgent that seismic drift limits are tightened in high-seismicity regions worldwide.

Keywords

Priority index, wall index, column index, drift, nonstructural damage, peak ground velocity

Date received: 14 July 2023; accepted: 9 October 2023

Background

In 1923, the Great Kanto Earthquake caused widespread devastation in Tokyo. Nevertheless, buildings designed by T. Naito performed well (Shiga et al., 1968). Damage caused by the 1933 Long Beach Earthquake prompted G. Howe (1936), an American architect, to study the work of Naito and to try to communicate his ideas to American engineers. Naito was emphatic in recommending the use of structural walls to make buildings stiff. Nevertheless, the American profession focused on the then-recently-discovered acceleration spectrum and did not follow that advice. The first codes for seismic design published in California in the 1950s clearly favored moment-resisting frames over structural walls. The rest of the world, except Chile and Japan, followed that example. The first seismic code for Turkey was published in 1940 (T.C. Bayındırlık Bakanlığı, 1940) adopting the Italian code of the time. The San Fernando Earthquake of 1971 showed that, without detailing to produce ductility (i.e. deformability), the moment-resisting frame was inadequate (Fintel, 1991). Most countries have since emphasized detailing for ductility instead of imposing more stringent drift limits despite Naito's and later M. Sozen's advice. As early as 1980, Sozen (1980) demonstrated—through controlled experiments and analysis—that the focus of earthquake-resistant design should be on drift instead of acceleration and force. Field work by Hassan and Sozen (1997) demonstrated the critical relevance of structural robustness in absence of good detailing. A century after Kanto, we are still paying the consequences of the lack of emphasis on building stiffness in design. Competent detailing can help avoid collapse, but (1) it is difficult to achieve in the absence of strict quality control, and (2) it does not help control drift. Excessive drift, in turn, causes (1) widespread damage to partitions, facades, finishes, and other nonstructural building components, (2) instability, and/or (3) failures in elements built without the mentioned quality control or with untested details.

Drift is driven by initial period and ground-motion intensity. It is impossible to control the latter, and, therefore, the only way to control drift is through period. In cast-in-place reinforced concrete (RC) buildings without dampers and isolation devices, the simplest way to control period is through controlling stiffness. Increases in mass associated with increases in stiffness are seldom critical. The corresponding increases in cost are not drastic either, especially if structural walls are used (García et al., 1996). Some authors advocate increasing longitudinal reinforcement ratios to increase stiffness. It is not clear that increases in reinforcement always lead to reductions in drift (Pujol et al., 2022; Shah, 2021).

Introduction

In a mission led by Committee 133 of the American Concrete Institute (ACI, 2023) nearly 250 buildings were surveyed by engineers and researchers from a wide consortium of entities (Table 1) to try to explore whether general trends could be observed between the frequency of damage and overall structural properties. The survey followed the methods and ideas proposed by Hassan and Sozen (1997). The response of a building to an earthquake is the intersection of effects from a large number of factors including type and extent of the rupture, site properties, distance to the fault line, structural configuration, reinforcement detailing, material properties, workmanship, quality control, and so on. Nevertheless, in that complex phenomenon, overall trends between key structural properties and building performance are plausible. This study focuses on testing whether structural robustness, expressed in terms of relative cross-sectional areas of structural walls, columns, and—in general—overall stiffness, may have correlated with performance of building structures shaken by the Earthquakes of February 2023 in Turkey. The focus of the investigation was on cast-in-place RC multistory buildings that were neither directly above the fault rupture, nor affected by liquefaction or foundation failures. Neither of these factors caused widespread damage in the cities visited, as far as the surveyors could see.

The earthquakes

Two main earthquakes affected southern Turkey and northwestern Syria on 6 February 2023: one quake with $M_w = 7.8$ with an epicenter near Pazarcik (US Geological Survey (USGS), 2023a), and one more quake, 9 hours later, with $M_w = 7.5$ with the epicenter near Elbistan (USGS, 2023b).

Figure 1 illustrates the locations of surveyed cities (blue symbols) and the intensities of the motions registered by instruments in or near them (red symbols). Intensity is represented in this figure in terms of displacement spectra obtained for linear single-degree-of-freedom systems (SDOFs) with a damping ratio of 5%. Black and gray straight lines represent the design basis earthquake (DBE) and the maximum considered earthquake (MCE) specified with the current Turkish design standards for each location. They are plotted against linear spectra obtained from acceleration records reported by the Turkish Disaster and Emergency Management Authority (AFAD-Afet ve Acil Durum Yonetimi Baskanligi) (2023). In most

Table 1. Participating institutions.

Type	Entity
Technical Society	ACI, Committee 133
Professional Association	ASCE
Governmental Agency	NIST
Academic Institutions	University of Canterbury; Purdue University; Izmir Institute of Technology; Dicle University; Hacettepe University; Harran University; Izmir University of Economics; Eskisehir Osmangazi University; University of Kansas; University of Nebraska at Lincoln
Consulting Companies	Wiss, Janney, Elstner Associates; Earthquake Solutions

ACI: American Concrete Institute; ASCE: American Society of Civil Engineers; NIST: National Institute of Standards and Technology.

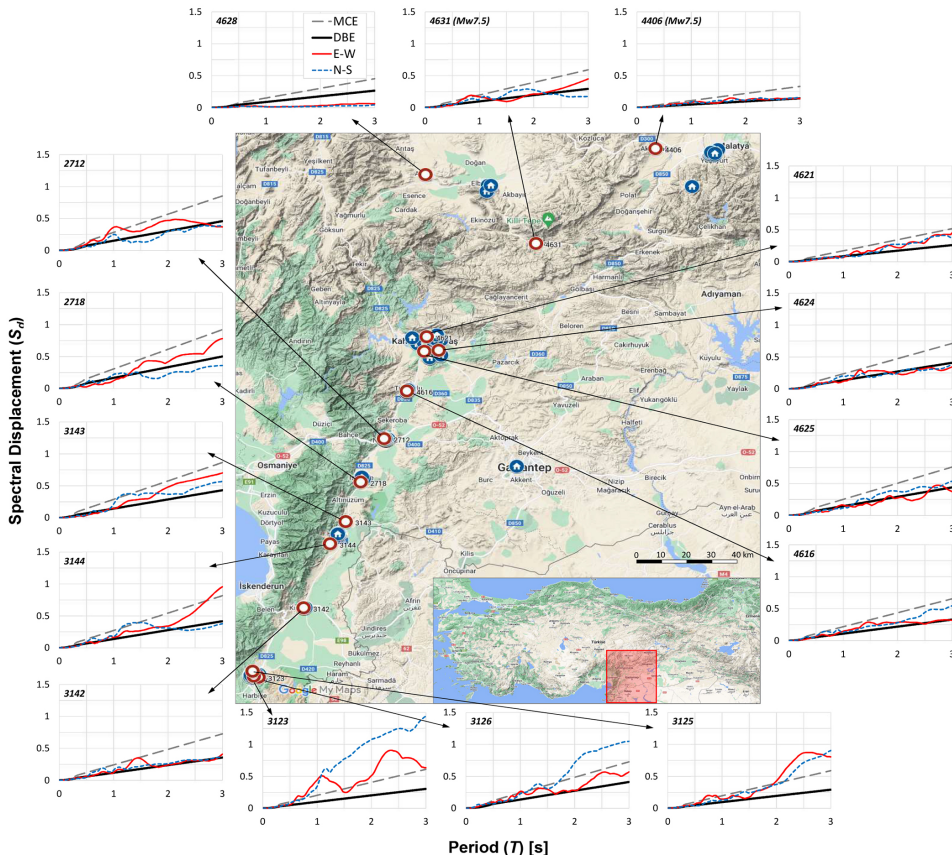


Figure 1. Affected area and the displacement demands of the recorded ground motions (red lines are for the “east-west (E-W)” direction, and the blue lines are for the “north-south (N-S)” direction) in comparison with current Turkish seismic regulation spectra.

cases, the DBE motion was exceeded, and near Antakya, even the MCE motion defined as the 2475-year return period event was exceeded for periods exceeding 0.6 s.

The average slope of the most intense displacement spectrum in Figure 1 (corresponding to the N-S direction in Antakya, station 3123) was nearly 50 cm/s. That is consistent with a value of peak ground velocity (PGV) of nearly $50 \times 8/3 \cong 130$ cm/s (Pujol et al., 2022). For many decades, buildings in highly seismic areas around the world were designed for values of peak ground acceleration (PGA) = 0.5g and peak ground velocity $PGV \cong 50$ cm/s, and a displacement spectrum with a slope approaching approximately 20 cm/s for 5% damping. The ground-motion intensity in some of the affected areas was demanding and higher than what the design spectra implied. Engineers should bear in mind the difficulty of predicting earthquakes and be aware that design spectra are not necessarily conservative.

Survey method and definitions

A total of 322 reinforced concrete buildings in the cities of Antakya, Islahiye, Hassa, Kirikhan, Nurdagi, Turkoglu, Gaziantep, Kahramanmaras, Malatya, and Elbistan were surveyed between 25 March and 6 April 2023. Complete sets of the parameters described

here were obtained for 242 of those 322. Survey teams consisted of three to four members each including researchers, engineers, architects, and engineering students. In total, approximately 40 people participated in the survey. At least one person in each team had previous experience in classifying earthquake damage. Surveying each building lasted roughly 1 to 3 hours. Each team, on average, surveyed 3–5 buildings per day. No clear signs of liquefaction or foundation problems were observed in the buildings surveyed.

Surveyed buildings were selected based on accessibility, size, age, and complexity. No effort was made to select buildings on the basis of their damage level, although buildings that were judged to be unsafe to enter were not surveyed. Most surveyed buildings had been constructed after 2000. Some effort was invested to survey taller buildings and buildings with more structural walls. The following information was collected for each building: Height; age; number of stories; location of the building; the presence of captive columns, soft stories, or irregularities; cross-sectional dimensions of columns and orientations, structural, and nonstructural walls; approximate floor plan dimensions; the presence of regular beams deeper than slabs (vs shallow-beam floor systems called “asmolen” frames); photographs; and damage classification.

Structural damage was classified as

- *None*
- *Light* (hairline cracks in RC walls, beams, or columns)
- *Moderate* (cover spalling or wider cracks in RC walls, beams, or columns)
- *Severe* (bar buckling, disintegration of the concrete core, or bond-splitting failure in RC walls or columns)
- *Critical* (widespread severe damage affecting a number of columns and/or structural walls to the point that the building was deemed to be likely to collapse in an aftershock)
- *Collapse* (loss of elevation of one or several floors).

Nonstructural damage was classified as

- *None*
- *Light* (hairline cracks or light flaking of plaster)
- *Moderate* (cracks in partition walls and joints or flaking of large pieces of plaster)
- *Severe* (wide and through cracks in partition walls and joints)
- *Collapse* (complete or partial collapse of partition walls).

The collected data are public, maintained by ACI Committee 133, and available here:

[https://www.dropbox.com/sh/6cmdgdn82n9ufxr/AACt-1rberSKM4fFFaDeL3_5a?dl = 0](https://www.dropbox.com/sh/6cmdgdn82n9ufxr/AACt-1rberSKM4fFFaDeL3_5a?dl=0)

For each building, data were collected at the “critical floor level” defined as the level deemed by surveyors in the field to produce the lowest values for the following calculated parameters:

1. *Column Index* = CI = sum of $1/2$ of cross-sectional column areas at the critical floor level divided by total floor area above the critical floor level.

2. *Wall Index* = WI = sum of cross-sectional RC wall areas and 1/10 of masonry infill areas at the critical floor level divided by total floor area above the critical floor level. The wall index (WI) is calculated for the principal floorplan direction producing the smallest value.
3. *Column Density* = CD = sum of cross-sectional column areas at the critical floor level divided by the typical floor plan area.
4. *Wall Density* = WD = sum of cross-sectional RC wall areas and 1/10 of masonry infill areas at the critical floor level divided by typical floor plan area. Wall density is calculated for the principal floorplan direction producing the smallest value.

Largely, the critical floor level was considered to be the ground level. In buildings with podiums (i.e. lower stories with larger floor plans), survey teams decided in the field whether the first level above the podium could be deemed more relevant than the ground level. In all cases, the area above the critical level refers to areas of elevated slabs above said level, including balconies and overhangs. This definition is an attempt to produce a value proportional to “seismic mass.” In buildings with penthouses, the area of the penthouse was estimated (from elevation, satellite, or drone views), and a fraction of the typical floor area was added to the total floor area above the critical level. Other cases needing judgment calls from the survey teams to define total floor area included buildings with partial height basements, founded on slopes, or with light wooden or metal roofs. The survey method could be and has been applied elsewhere, but it is targeted to low- and mid-rise RC building structures and has not been tried nor adapted for other types of structures.

Observations

Structural systems

RC frames with beams deeper than slabs. Most surveyed structures had RC frames with RC or masonry infill walls located around an elevator shaft. Where beams deeper than the slabs were observed, they were typically framed into columns. But frames tended to have highly irregular column lines across floor plans (Figure 2) with columns not always aligned along straight gridlines and, in some instances, with beams framing into other beams instead of columns. Some buildings also had upper columns or walls which did not reach the foundation but were supported instead by transfer beams. The longitudinal axes of beams were often offset from the longitudinal axes of supporting columns. Along perimeters, these offsets were introduced to align exterior beam and column faces. Gemici (2019) showed that the described irregularities can cause increases in the initial period of up to 50%.

RC frames with shallow beams. In nearly 25% of the structures surveyed, the flooring system consisted of “shallow beams” and one-way joists. Typical dimensions of shallow-beam frames that are often called ribbed slabs in the United States (called “asmolen” or “disli doseme” systems in Turkey) are shown in Figure 3 together with a photograph of such a frame during demolition (building located in Nurdagi, Gaziantep). In these frames, beam depths did not exceed the depths of the joists (typically 30–35 cm) in the interest of producing a flat ceiling. Joists were formed during casting by using rows of hollow concrete masonry units (CMU) that remained in place and became part of the floors.

Observations are organized in Figure 4 to show the distribution of damage classifications for surveyed buildings with regular and shallow-beam frames. Evidently, the frequency of severe damage was higher among buildings with shallow beams (88% compared

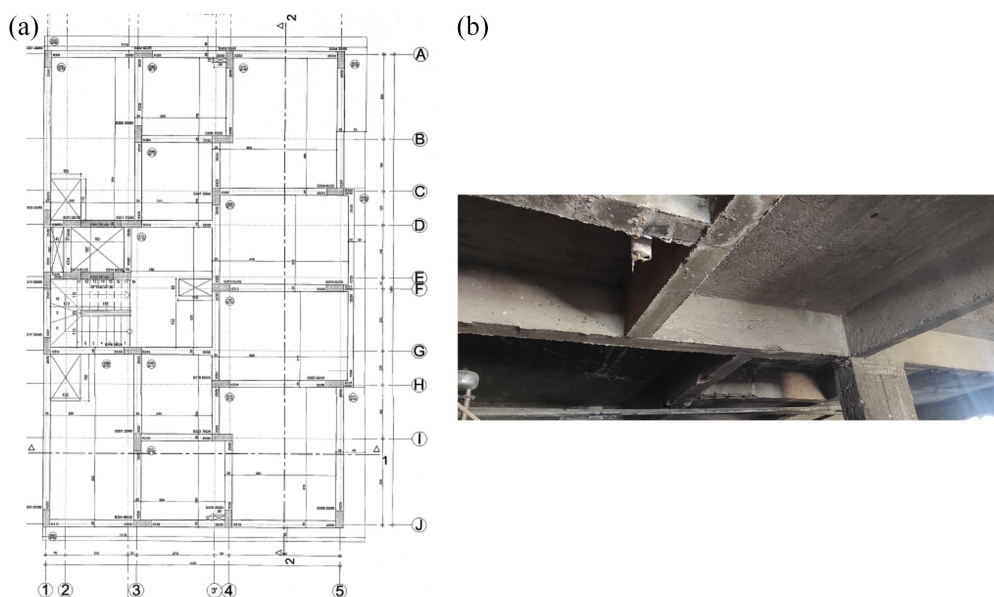


Figure 2. Irregular framing examples: (a) floor plan and (b) floor soffit.

with 59% for frames with regular beams—deeper than slabs). These observations are consistent with the findings of Dönmez (2015), who showed that frames with shallow beams have lower stiffness and higher seismic drift demands.

Wall construction. A limited number of buildings were observed to have been built with a method known as “tunnel-form construction” (illustrated here: https://youtu.be/_j-FRe8Ay9s). These structures tend to have abundant structural RC walls (occupying 2% to 6% of a typical floor plan). They were observed to be configured in one of two ways: (1) including similar amounts of wall in each principal floor plan direction, or (2) with most walls oriented in a single floor plan direction. The latter cases were observed to have more signs of structural distress, whereas buildings with well-distributed walls in both orthogonal plan directions commonly performed well, exhibiting only light damage (Figure 5).

Structural configuration issues

The following problems related to the configuration of the surveyed structures were observed. The numbers on the figures in Supplementary Material 1 correspond to the items listed below:

1. Lack of structural walls (Supplementary Material 1);
2. Irregular column lines (Figure 2);
3. Differences in lateral stiffness in the two principal floor plan directions;
4. Insufficient separation between buildings leading to pounding;
5. Beam axes offset from column axes (Supplementary Material 1);
6. Beams framing into other beams instead of columns (Supplementary Material 1);
7. Short beams (not detailed to resist high shear forces) (Supplementary Material 1);

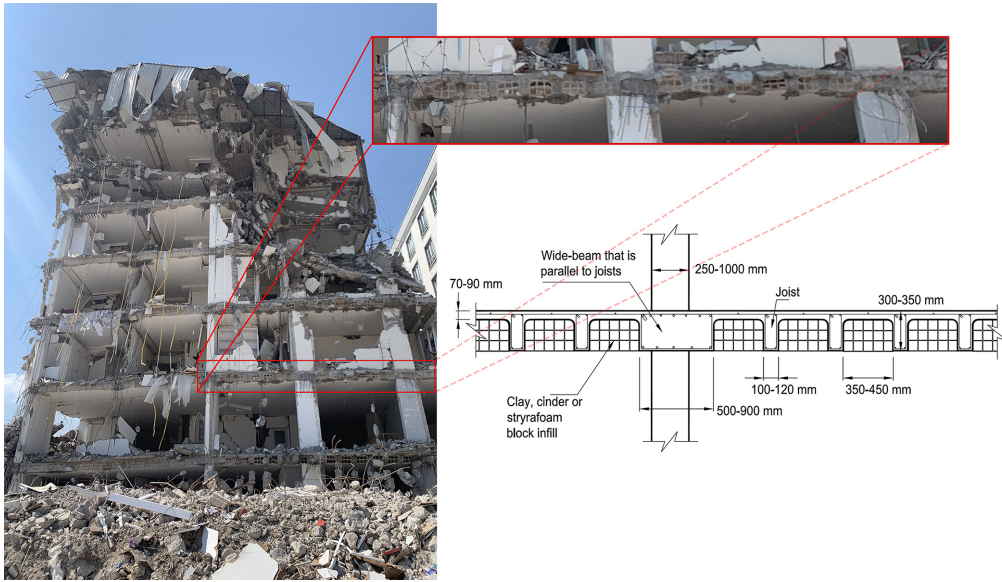


Figure 3. Partially demolished reinforced concrete frame with shallow beams and typical dimensions of one-way joist-slab shallow-beam frames in Turkey.

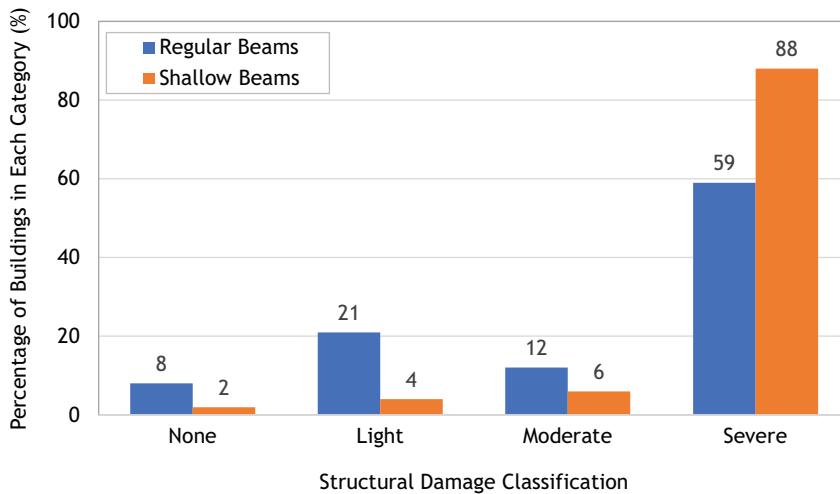


Figure 4. Damage frequency observed in reinforced concrete frames with regular beams and shallow beams (critical and collapsed structures are included within the bin labeled “severe”).

8. Columns discontinuous in elevation (i.e. columns supported by transfer girders);
9. Soft stories caused by dense masonry infill concentrated in upper floors and open-plan ground stories (Supplementary Material 1);
10. Lack of beams (deeper than slabs) (Supplementary Material 1); and
11. Heavy overhangs (Supplementary Material 1).



Figure 5. Wall structures with similar amounts of wall in each principal floor plan direction: (a) typical floor plan and (b) example of wall building built by Housing Development Administration of Turkey (TOKI-Toplu Konut Idaresi Başkanlığı) at Dulkadiroglu, Kahramanmaraş.

Table 2. Column and wall indices for the surveyed buildings.

	CI (%)	WI (%)	PI = CI + WI (%)	CD (%)	WD (%)
M	0.10	0.07	0.17	1.3	0.46
SD	0.06	0.09	0.09	0.61	0.56

CI: column index; WI: wall index; PI: priority index; CD: column density; WD: wall density; SD: standard deviation; M: mean.

CD and WD are defined with the same numerators as WI and CI and typical floor area as denominator.

Quantitative evidence collected in Turkey shows that the most salient issues that affected RC buildings in the southeast region of Turkey extending from Antakya to Malatya were inadequate structural stiffness and deficient reinforcement detailing. It was apparent in the field that buildings with flexible lateral force-resisting systems performed worse than robust buildings with structural walls in both principal plan directions. In general, the surveyed buildings were found to have low amounts of walls and columns as reflected by the indices given in Table 2.

For context, consider that Hassan and Sozen (1997) recommended a minimum value of CI+WI of 0.25% (to prioritize retrofit efforts). Consider also that buildings in Chile have been reported to have much higher wall areas, with WI on the order of 0.3% for 10-story buildings (Figure 3.10 of the work by Riddell et al., 1987). Other comparisons with indices from other regions are provided in the “Comparisons with Previous Observations” section.

Detailing issues

Problematic reinforcing bar details were repeatedly observed by the reconnaissance teams. Several are described below and classified based on whether the details comply with ACI 318-19 (2019) (or similar building codes). No attempt is made to attribute responsibility

for the presence of details that did not comply with building regulation requirements. Photographs of the following detailing issues that do not comply with building regulation requirements are provided online with Supplementary Material 2. The numbers on the figures in Supplementary Material 2 correspond to the items below.

1. *Concrete cover or longitudinal bar spacings smaller than required:* This defect was observed in elements affected by cover spalling. Both spalling and small cover can affect the bond between the longitudinal bars and concrete, especially along lap splices.
2. *Lack of 135° hooks (90° hook–ties):* 90° tie hooks were often observed where longitudinal bar buckling and damage to the core concrete had occurred.
3. *Widely spaced transverse reinforcement around small-diameter longitudinal bars:* Hoops or ties spaced at 15 cm or wider spacings were frequently observed. With longitudinal bars having diameters d_b of 12 to 18 mm, these spacings exceeded $8d_b$. ACI 318-19 (2019) limits hoop spacing to not more than $6d_b$ in special moment frames and boundary elements of special structural walls with Grade 420 longitudinal bars. Widely spaced hoops coincided with buckled longitudinal bars and core damage.
4. *Widely spaced transverse reinforcement at cold joints:* Longitudinal bar buckling was observed at the bases of columns with acceptable confinement elsewhere because the space between the topmost foundation hoop and the bottommost column hoop was excessively large. Care during construction is necessary to ensure proper hoop spacing across cold joints.
5. *Lap splices at column bases:* Longitudinal bars were often lap spliced at the bases of columns, which ACI 318-19 (2019) prohibits in seismic design categories (SDC) D, E, and F. Aside from being prone to abrupt failure, lap splices at column ends concentrate strains at member ends where buckled and fractured bars were often observed.
6. *Lap splices at wall bases:* Since 2019, ACI 318 prohibits lap splices in wall boundary-element longitudinal reinforcement near sections where yielding is expected. Lap splices are prone to abrupt failure, but even when they do not, lap splices cause sharp curvature and strain concentrations at their ends. Photographs 6a and 6b in Supplementary Material 2 show (1) a 2.7-m-long wall with lap splices starting 0.7 m above the top of the foundation; wall damage concentrated within a narrow band near the wall base, and (2) a 2.2-m-long wall with longitudinal bar lap splices beginning just above the foundation; a prominent horizontal crack with bar buckling and severe concrete damage occurred at the top of the splices.
7. *Lack of confinement for column and wall longitudinal bars inside foundation:* Several examples were observed of buckled column and wall longitudinal bars below the top of the foundation or in grade beams. This occurred near foundation edges where the bars were not confined. This is a life-safety issue because the buckled bars can cause columns to move laterally and no longer bear on the foundation (Supplementary Material 2, Photograph 7b). This detail is prohibited in ACI 318-19 Section 18.13.2.4 for longitudinal bars of columns and boundary elements of special structural walls in SDC D, E, or F. ACI 318 and other standards should apply the requirement to confine bars within foundations to intermediate moment frame columns.
8. *Lack of crossties in columns and structural walls:* buckled longitudinal bars and severely damaged concrete were observed in columns and walls without through-

- thickness cross-ties. Long hoop legs or horizontal web bars did not provide adequate confinement for these load-bearing RC members.
9. *Offset-bent longitudinal bars (so-called “Dog-Leg” detail) at the base of columns/walls:* Column and wall longitudinal bar buckling and fracture were frequently observed at the top of a foundation where an offset-bent detail was used (where a longitudinal bar extending from the foundation is bent toward the center of the section and then bent again to orient the tail parallel to the longitudinal bars for splicing). Although offset-bent longitudinal bars are permitted, the observed slope of the inclined portion typically did not comply with ACI 318-19 (2019) requirements.
 10. *Nonstructural element penetrations through structural elements (beams, columns, walls, and slabs):* Penetrations through structural elements are permitted if detailed appropriately. Ad hoc penetrations, like that shown in Supplementary Material 2, Photograph 10, did not satisfy building standard requirements and were often associated with concrete cracking and spalling.
 11. *Masonry infill walls not isolated from the structure or mechanically anchored to the surrounding structure:* Brittle infill walls made with hollow clay tile, cinder blocks, and aerated autoclaved concrete blocks (called “gazbeton” in Turkey) and butted directly against the structure were observed to fail even in buildings without perceptible structural damage. Numerous buildings without structural damage but widespread damage to brittle partitions were evacuated and reportedly scheduled for demolition.

Photographs of the following detailing issues that appear to comply with ACI 318-19 (2019) building code requirements are provided in Supplementary Material 3. The numbers on the figures in Supplementary Material 3 correspond to the items below. Observed detailing issues that comply with ACI 318-19 (2019) requirements:

1. *Unconfined beam bars in beam-column joints:* Supplementary Material 3 shows joints with unconfined outermost beam longitudinal bars outside the column core. A vertical splitting plane caused cover spalling, leaving the exposed beam bars unrestrained and unbonded. For special moment-resisting frames, ACI 318-19 (2019) requires beam longitudinal reinforcement outside the column core to be confined, but this requirement does not apply to frames not designated as part of the seismic-force-resisting system.
2. *Bar termination locations in beams:* Wide cracks and spalling were often observed where bottom beam longitudinal bars were terminated. The problem appeared to be most prevalent in shorter beams, beams with bars terminating within approximately two member depths from the column face, and in beams with light transverse reinforcement. ACI 318-19 (2019) does not appear to address potential problems related to the termination of bottom beam reinforcement close to column faces in frames resisting earthquake demands.
3. *Damage to short beams between walls (not detailed as coupling beams):* Heavy damage was observed in short beams linking structural walls. These beams did not have diagonal bars and appeared not to have been classified as part of the seismic-force-resisting system. Nevertheless, the extent of damage contributed to concerns among residents and, often, was reportedly a basis to justify demolition.

The perception of the surveying teams is that correcting the listed detailing issues would have reduced the observed damage and could have prevented several collapses. Nevertheless, correcting these details would not have reduced damage to nonstructural elements or prevented collapses attributable to excessive drift.

Issues with nonstructural elements

Severe damage to nonstructural elements was widespread, often making structures unusable and unsafe even when structural damage was light. Approximately 90% of surveyed buildings with masonry infill walls were classified as having either severely damaged or collapsed partitions and facades. There were very few instances of studded gypsum-board (drywall) partitions, and these partitions were observed to be (1) less prone to complete disintegration and collapse, and (2) less dangerous to building occupants. Use of studded gypsum board or other lightweight partitions that are restrained out-of-plane while allowing for in-plane displacement—relative to the structure—is strongly recommended. Where masonry infill walls are used, they should be separated from the frame but reinforced and restrained against out-of-plane movement. Examples of damage to reinforced concrete stairs, which was widespread, are provided online in Supplementary Material 4. Stairs are an essential means of egress, and the extent and prevalence of severely damaged stairs are a concern. Typical details were inadequate for accommodating large story drift demands.

Correlations between damage and intensity measures

Table 3 and Figure 6 show damage frequencies (% of inspected buildings observed to have damage) organized against several intensity measures:

PGA;

PGV;

Spectral displacement (S_d) for periods (T) = 0.3 s and 1 s, and a damping ratio of 2%;

Spectral velocity (S_v) for periods (T) = 0.3 s and 1 s, and a damping ratio of 2%;

Spectral acceleration (S_a) for periods (T) = 0.3 s and 1 s, and a damping ratio of 2%.

Estimates of these intensity measures were obtained using accelerations recorded at the ground-motion recording stations closest (<5 km) to inspected areas. An exception was made for Malatya, where the closest station was approximately 25 km from the city center. In locations with more than one station within 5 km, the intensity measures considered are means of the peak values from all stations within 5 km. For Göksun, Elbistan, and Malatya, intensity measures for the $M_w = 7.5$ earthquake (the second largest earthquake on 6 February 2023) were used, because they are higher than those for the $M_w = 7.8$ earthquake. For other locations, intensity measures correspond to the $M_w = 7.8$ motion.

The listed damage frequencies were obtained from two sources: reports from thorough surveys commissioned by the Turkish government, and the survey presented in this document, (herein referred to as the ACI-133 survey). In the latter case, damage frequencies in Table 3 and Figure 6 refer exclusively to buildings with critical damage or collapse as defined above. In the former case, the surveyors working for the government used a damage scale and criteria different from those described here. The frequencies reported for their survey refer to buildings classified as having “severe” damage or collapse.

Table 3. Damage frequencies and intensity measures.

City/district	Damage frequency (%)	PGA (g)	PGV (m/s)	$S_{d0.3}$ (m)	$S_{v0.3}$ (m/s)	$S_{a0.3}$ (g)	S_{d1} (m)	S_{v1} (m/s)	S_{a1} (g)
Ministry survey									
Altınözü, Hatay	26	0.53	0.54	0.04	0.74	1.57	0.18	1.12	0.72
Andırın, Kahramanmaraş	12	0.16	0.15	0.01	0.19	0.40	0.03	0.16	0.10
Antakya, Hatay	50	0.54	1.04	0.04	0.81	1.73	0.45	2.84	1.82
Arsuz, Hatay	7	1.34	0.65	0.07	1.37	2.93	0.21	1.31	0.84
Belen, Hatay	9	0.38	0.51	0.03	0.59	1.27	0.13	0.79	0.50
Ceceli, Kahramanmaraş	44	0.68	0.96	0.07	1.54	3.29	0.19	1.22	0.78
Defne, Hatay	40	1.37	1.70	0.16	3.30	7.05	0.55	3.43	2.20
Dörtöyl, Hatay	7	0.25	0.40	0.02	0.33	0.71	0.16	1.02	0.66
Göksun, Kahramanmaraş	39	0.64	1.71	0.02	0.51	1.09	0.18	1.13	0.72
Hassa, Hatay	28	0.65	1.12	0.04	0.85	1.82	0.23	1.41	0.91
İskenderun, Hatay	14	0.13	0.28	0.01	0.16	0.34	0.09	0.54	0.34
İslahiye, Gaziantep	27	0.66	1.13	0.05	1.11	2.37	0.31	1.93	1.23
Kırıkhan, Hatay	34	0.73	1.20	0.05	1.07	2.28	0.31	1.92	1.23
Nizip, Gaziantep	4	0.17	0.13	0.01	0.18	0.39	0.07	0.45	0.29
Nurdağı, Gaziantep	50	0.60	1.09	0.05	1.03	2.21	0.48	3.01	1.93
Pazarcık, Kahramanmaraş	31	0.63	1.22	0.03	0.68	1.46	0.24	1.52	0.97
Samandağ, Hatay	38	0.22	0.79	0.02	0.35	0.74	0.22	1.40	0.90
Türkoğlu, Kahramanmaraş	28	0.46	0.56	0.04	0.87	1.85	0.16	1.02	0.65
ACI-133 survey									
Antakya, Hatay	26	0.99	1.33	0.06	1.29	2.75	0.35	2.20	1.41
Elbistan, Kahramanmaraş	22	0.40	0.93	0.03	0.57	1.21	0.21	1.29	0.83
Hassa, Hatay	32	0.59	1.29	0.04	0.75	1.60	0.23	1.45	0.93
Kahramanmaraş (central)	35	0.41	0.61	0.03	0.56	1.19	0.22	1.36	0.87
Kırıkhan, Hatay	17	0.75	0.86	0.05	1.07	2.29	0.19	1.21	0.77
Malatya (central)	25	0.45	0.35	0.02	0.46	0.98	0.14	0.86	0.55
Nurdağı, Gaziantep	38	0.60	1.09	0.05	1.03	2.21	0.48	3.01	1.93
Türkoğlu, Kahramanmaraş	19	0.68	0.96	0.07	1.54	3.29	0.19	1.22	0.78

PGA: peak ground acceleration; PGV: peak ground velocity; ACI: American Concrete Institute.

The survey commissioned by the government covered a larger geographical area than the ACI-133 survey did. The data presented here for the government survey refer only to neighborhoods within 5 km from ground-motion recording stations. The ACI-133 survey did not cover entire cities or entire neighborhoods. Areas identified with the same city or district name (e.g. Antakya, Hatay) for both surveys do not always refer to the same geographical area, and, therefore, the reported mean intensity measures differ between the two surveys.

In general, spectral ordinates for $T = 0.3$ s did not produce better correlations with frequency of damage than spectral ordinates for $T = 1$ s. Spectral accelerations (S_a) and spectral velocities (S_v) for $T = 1$ s produced correlations comparable with the correlations seen for spectral displacement (S_d) at 1 s. PGV produced correlations better than those for PGA, and similar to those for S_d at 1 s. Given the mentioned differences in the surveys, a good match between the two sets of data on damage frequency was not expected. What matters more is whether both sets of data produce the best correlations with observed damage for the same intensity measure(s). They did, with PGV and S_d at 1 s producing better correlations for both surveys. PGV has the advantage of being simple. Recall that PGA often requires “corrections” or has to be expressed in terms of an “effective” value

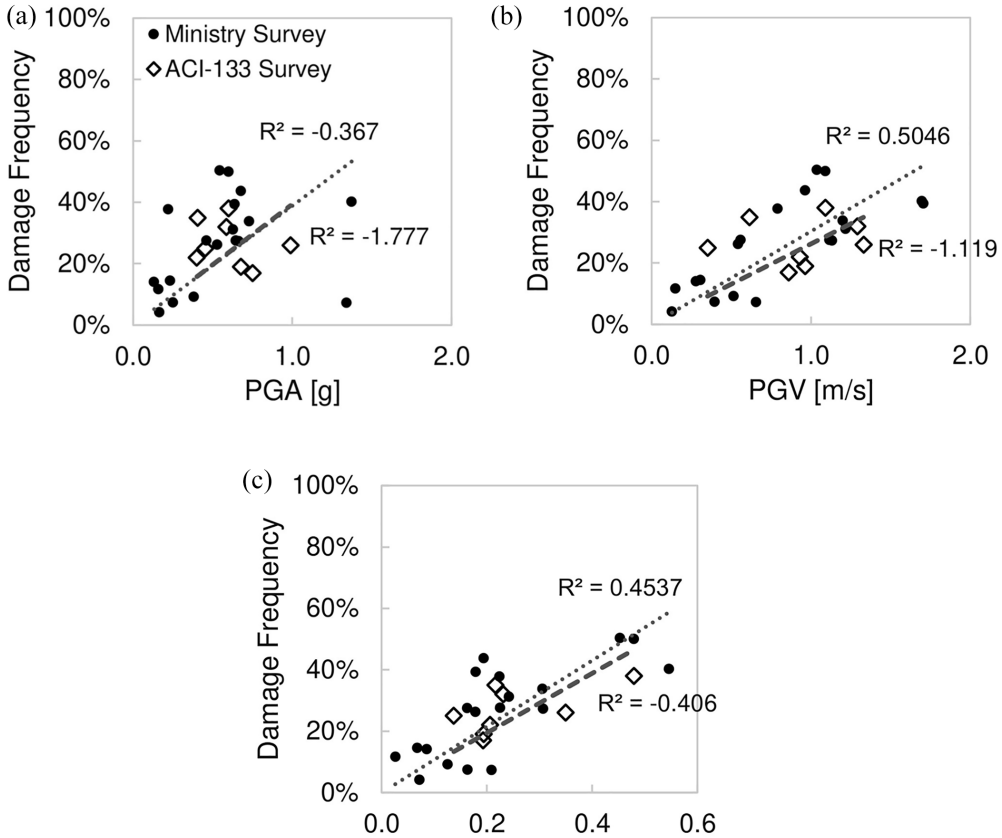


Figure 6. Correlations between damage intensities and intensity: (a) peak ground acceleration as the intensity measure, (b) peak ground velocity as the intensity measure, and (c) spectral displacement (S_d) for a period of 1 s and damping ratio of 2%.

produced mostly by judgment. Here, no attempt was made to modify the values of PGA reported by AFAD (2023). PGV was obtained by integrating the published acceleration records. The records were baseline corrected and filtered (to remove frequencies outside 0.025–40 Hz range) by AFAD.

Correlations between damage and robustness measures

Figure 7 shows CI versus WI for buildings from all the visited cities. A line at $WI = (0.25\% - CI)$ similar to what Hassan and Sozen (1997) recommended (1) would fall above most of the data points, and (2) reasonably bound the buildings observed to have severe damage. Figure 8a and 8b groups data by cities where the intensity of the ground motion was high (Nurdagi, Turkoglu, Kirikan, Hassa, Antakya, and Islahiye, where PGV exceeded 50 to 60 cm/s) and cities where the intensity was low (Gaziantep, Kahramanmaras, Malatya, and Elbistan, where PGV did not exceed 50 to 60 cm/s). The points representing buildings with severe damage are closer to the origin for the latter group of cities. In their cases, the line $WI = (0.2\% - CI)$ would be above most of the buildings observed to have severe damage. Nevertheless, the lack of data points with CI close to zero and $(1/8)\% < WI < 0.3\%$ in Figure 8b does not allow for a stronger statement.

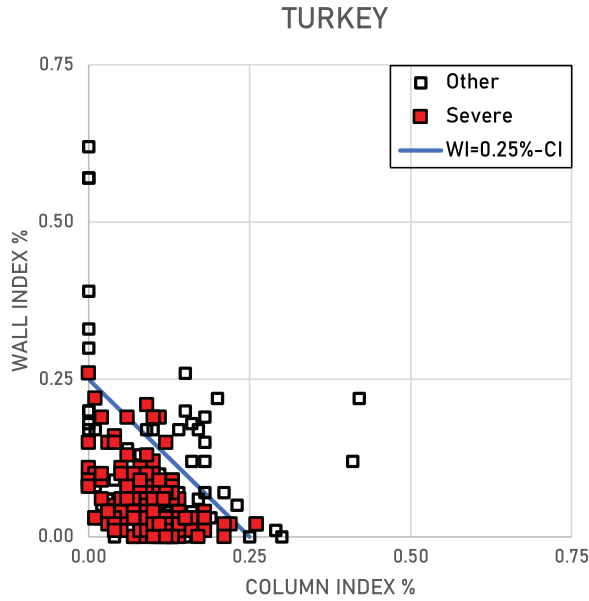


Figure 7. Column index versus wall index for buildings surveyed by ACI-I33 in 2023.

Figure 9 shows damage distribution versus priority index (PI), PI/S_a , and PI/S_d . S_a is expressed in g and calculated for $T = N/10$ and 2% damping for the station closest to each surveyed building. S_d is expressed in meters and is calculated for $T = N/10$ and 2% damping for the record obtained at the station closest to each surveyed building. In Figure 9b, the labels on the horizontal axis refer to

For $(CI + WI)/S_d$:

- 1 = $0.0 < (CI + WI)/S_d < 0.5$
- 2 = $0.5 < (CI + WI)/S_d < 1$
- 3 = $1 < (CI + WI)/S_d < 1.5$
- 4 = $1.5 < (CI + WI)/S_d < 3$
- 5 = $3 < (CI + WI)/S_d < 20$

For $(CI + WI)$:

- 1 = $0.00 < CI + WI < 0.10\%$
- 2 = $0.10 < CI + WI < 0.15\%$
- 3 = $0.15 < CI + WI < 0.20\%$
- 4 = $0.20 < CI + WI < 0.25\%$
- 5 = $0.25 < CI + WI < 1.00\%$

The chart in Figure 9a shows that the correlation between damage frequency (among surveyed buildings) and the sum $PI = WI + CI$ is not improved in a clear fashion if PI is divided by spectral acceleration (S_a) (in g) at a period $T = N/10$ ($N =$ number of stories).

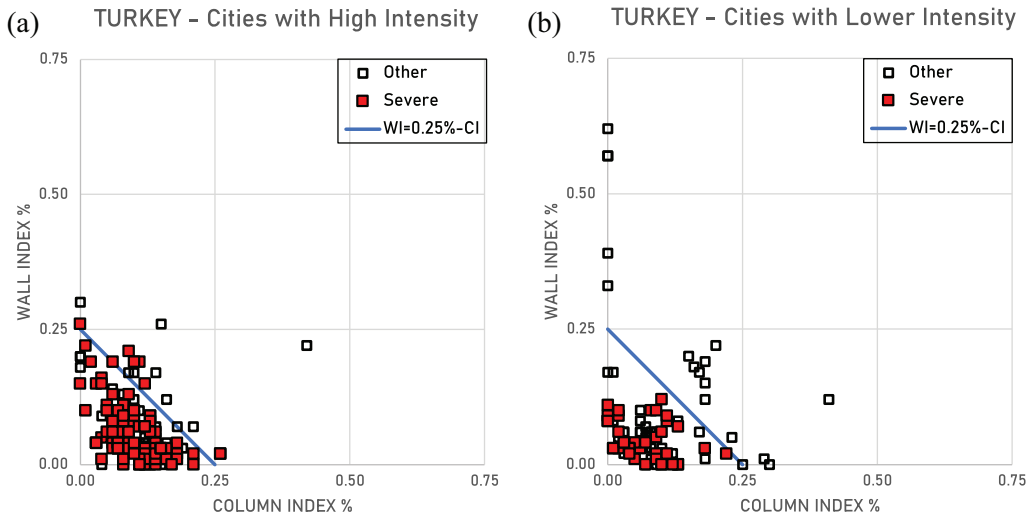


Figure 8. Data separated for cities subjected to (a) high and (b) low ground-motion intensities.

Figure 9b is similar to Figure 9a, except that it was produced by dividing PI by S_d (in m) instead of S_a (at $T = N/10$). The correlation between damage frequency and PI/S_d appears to be stronger than the correlation between damage frequency and PI . Values of S_a and S_d assigned to each building were obtained from the acceleration record obtained at the station closest to the building. The distances between buildings and stations were estimated using the Haversine formula. Buildings with no stations within 30 km were excluded from Figure 9.

Perhaps more interestingly, the points representing buildings with critical damage (as defined above) are quite close to the origin and the x-axis of the $WI-CI$ plot (Figure 10a). Approximately 96% of buildings classified as having critical damage had $WI \leq 0.1\%$. Wall density and column density (defined with the same numerators as WI and CI and typical floor area as denominator) did not help organize the data better (Figure 10b). Even though the WI and CI had been calibrated—until now—for buildings with 7 or fewer stories, the same observation is made for buildings with more than 7 stories. The evidence in this section confirms once more that $WI + CI$ can be used to prioritize retrofit efforts. It would seem imperative to start with all buildings with $WI < 0.1\%$ in zones where the expected demands (whether measured in terms of S_a , S_d , or PGV) are high.

Even though Hassan and Sozen's original proposal was to use the CI and WI to prioritize retrofit resources, the observations described here, and the historical comparisons presented in the next section suggest that the indices could be used to craft design criteria to produce more robust structures less prone to damage. The data above suggest that a design threshold referring exclusively to WI would be effective within the ranges of parameters considered. ACI 314R-16 (2016) Guide to Simplified Design for Reinforced Concrete Buildings indirectly recommends $WI > 0.2\%$ for buildings with $N \leq 5$. The observations presented suggest that this recommendation could be extended up to $N = 15$, resulting in a wall density $WD = 3\%$ at $N = 15$. As mentioned above, $WD = 3\%$ is the mean wall density dictated by Chilean traditions for $5 < N < 25$ (Riddell et al., 1987). The following section provides more context to judge the observations made in Turkey in 2023.

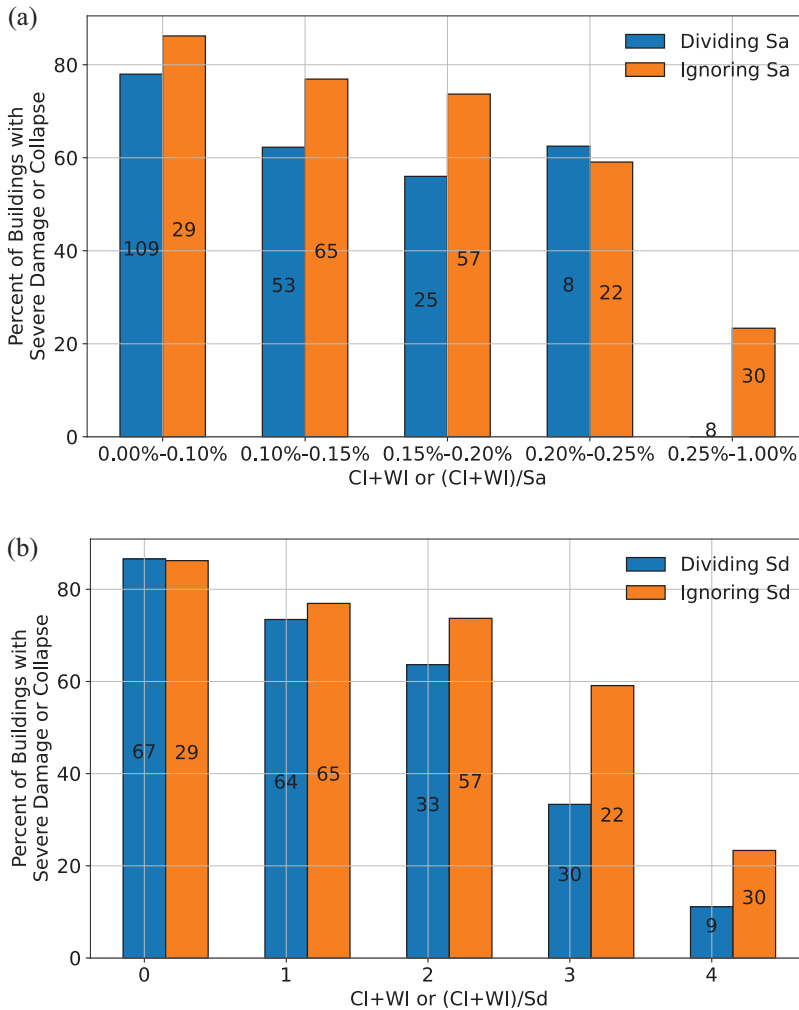


Figure 9. Damage distribution versus PI , PI/S_a , and PI/S_d : (a) damage distribution among surveyed buildings versus PI and PI/S_a , and (b) damage distribution among surveyed buildings versus PI and PI/S_d . PI : priority index.

Comparisons with other observations

CI and WI from 1639 buildings surveyed after 15 earthquakes, including the 2023 Turkey Earthquakes, have been collated to look for general trends and to provide a frame of reference to judge what occurred in Turkey in 2023. Table 4 lists the mean values of the WI , CI , and $PI = WI + CI$ calculated for each earthquake. Percentages of surveyed buildings classified as having severe damage or collapse and mean PGVs are also listed. Mean values of PGV range from 30 to 90 cm/s . Values of PGV listed for Haiti (2010) and Pohang (2017) are approximations obtained using reported modified Mercalli intensities (MMIs) and the scale proposed by Wald et al. (1999). Several of the earthquakes had a single ground-motion record available near the survey site (Bingol 2003; Chile 1985; Duzce 1999; Erzincan 1992; Peru 2007; and China 2008). In cases where several stations were available, the listed values are means corresponding to the stations deemed to be more

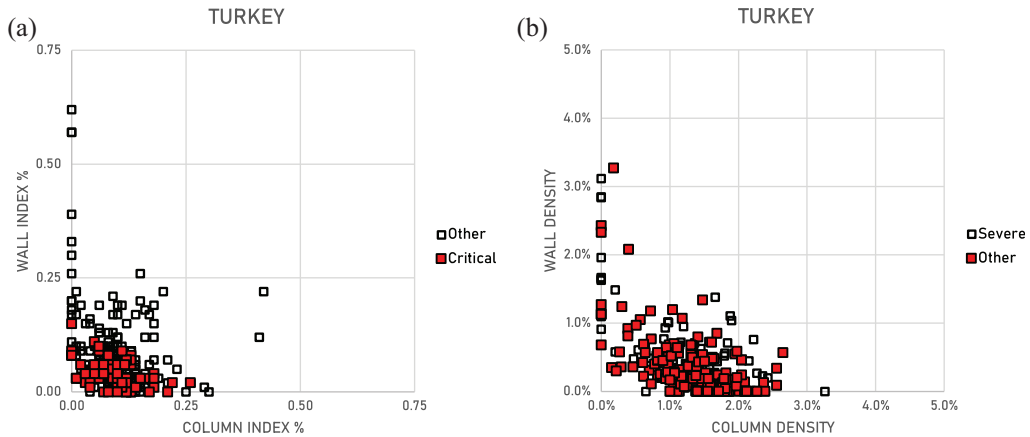


Figure 10. (a) Wall index versus column index for buildings with critical damage and (b) data organized as column density versus wall density.

Table 4. Observations from other earthquakes.

Earthquake	Year	Author/s	PGV (cm/s)	Buildings	Severely damaged buildings (%)	Average CI (%)	Average WI (%)	Average PI (%)
Japan	1968	Shiga (1977)	35	98	18	0.28	0.35	0.64
Chile	1985	Riddell et al. (1987)	35	144	2	0.02	0.35	0.37
Erzincan	1992	Hassan and Sozen (1997)	50	49	14	0.25	0.12	0.37
Duzce	1999	Gur et al. (2009)	50	210	26	0.28	0.04	0.32
Bingol	2003	Gur et al. (2009)	37	57	46	0.19	0.12	0.31
Peru	2007	Cuadra et al. (2013)	62	27	42	0.31	0.04	0.36
China	2008	Zhou et al. (2013)	30	116	22	0.14	0.08	0.22
Haiti	2010	O'Brien et al. (2011)	45 ^a	160	39	0.23	0.05	0.28
Christchurch	2011	Pledger et al. (2023)	65	24	46	0.05	0.09	0.14
Nepal	2015	Shah et al. (2017)	70	135	44	0.16	0.03	0.19
Taiwan	2016	Pujol et al. (2020)	45	103	22	0.26	0.09	0.34
Ecuador	2016	Villalobos et al. (2018)	55	172	45	0.22	0.03	0.25
Mexico	2017	Alcocer et al. (2020)	30	50	32	0.14	0.02	0.16
Pohang	2017	Sim et al. (2018)	45 ^a	71	45	0.21	0.08	0.29
Turkey	2023		90	223	65	0.10	0.07 ^b	0.17 ^c

PGVs: peak ground velocities; CI: column index; WI: wall index; PI: priority index.

^aEstimates of PGV for the 2017 Pohang and 2010 Haiti Earthquakes were estimated based on the MMI of VIII measured at the surveyed sites and the PGV-MMI relationships developed by Wald et al. (1999).

^bWI = 0.08 for buildings with 7 or fewer stories.

^cWI + CI = 0.2 for buildings with 7 or fewer stories.

representative. Surveyed buildings had 1 to 23 stories, with more than 90% of buildings having 7 or fewer stories. Surveys from 1992 onwards were conducted by teams trying to follow the damage classification scale presented here. Surveys from Chile 1985 and Japan 1968 were independent. In the latter case, *severe* damage refers to shear failure in columns. For Chile, *severe* simply refers to the top of a scale ranging from *none* to *severe* damage (Riddell et al., 1987). Figure 11 shows *WI* versus *CI* for all 1639 buildings. The mentioned

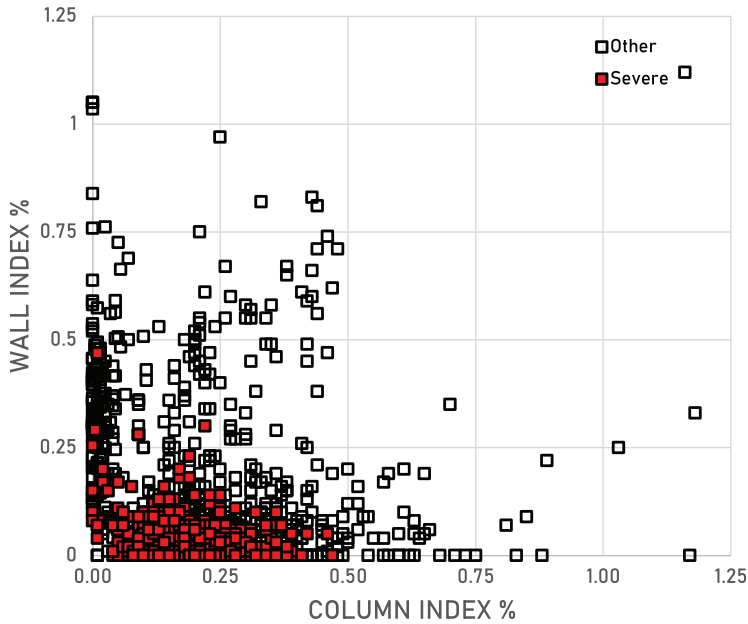


Figure 11. Column index versus wall index for 1639 buildings across 15 earthquakes.

differences among damage classification scales and methods are likely to contribute to the scatter in the data. Nevertheless, the results show a trend similar to the trend in Figure 7, with severely damaged buildings concentrated mostly in the area between the origin and the line $WI = (0.25\% - CI)$.

Figure 12a and b illustrates the percentage of surveyed buildings classified as having severe damage versus PI and WI . Fractions above bars refer to the number of buildings classified as having severe damage (numerator) and the total number of buildings in each bin (denominator). The illustrated data show that increases in PI and WI have been consistently associated with reductions in the numbers of buildings with severe damage. Less than 4% (9/245) of all surveyed buildings with $WI > 0.2\%$ had severe damage, compared with $\sim 40\%$ (563/1394) for $WI < 0.2\%$. Similarly, $\sim 12\%$ (66/541) of all surveyed buildings with $PI > 0.3\%$ had severe damage, compared with $\sim 46\%$ (508/1098) for $PI < 0.3\%$. Approximately 65% (90/139) of all surveyed buildings with a $PI < 0.1\%$ were classified as having severe damage. Approximately 90% (516/572) of all severely damaged buildings had a $WI < 0.1\%$.

Figure 12a and b make a direct comparison between buildings surveyed in Turkey in 2023 and other buildings surveyed. Both sets of data exhibit a reduction in severely damaged buildings as PI and WI increase. Nevertheless, the percentage of severely damaged buildings was noticeably higher in Turkey in 2023. This is likely due to the larger demands recorded in Turkey, with an average $PGV \sim 90 \text{ cm/s}$ across all the surveyed sites and the lack of robustness in the surveyed buildings. Only 7% (15/223) of buildings recently surveyed in Turkey had $PI > 0.3\%$, while the rest of the data set had 37% (526/1416) of buildings in that category. Similarly, $\sim 5\%$ (11/223) of buildings recently surveyed in Turkey had $WI > 0.2\%$, while $\sim 17\%$ (234/1416) of the buildings in the rest of the data set had $WI > 0.2\%$. These figures suggest that buildings recently surveyed in Turkey were, on

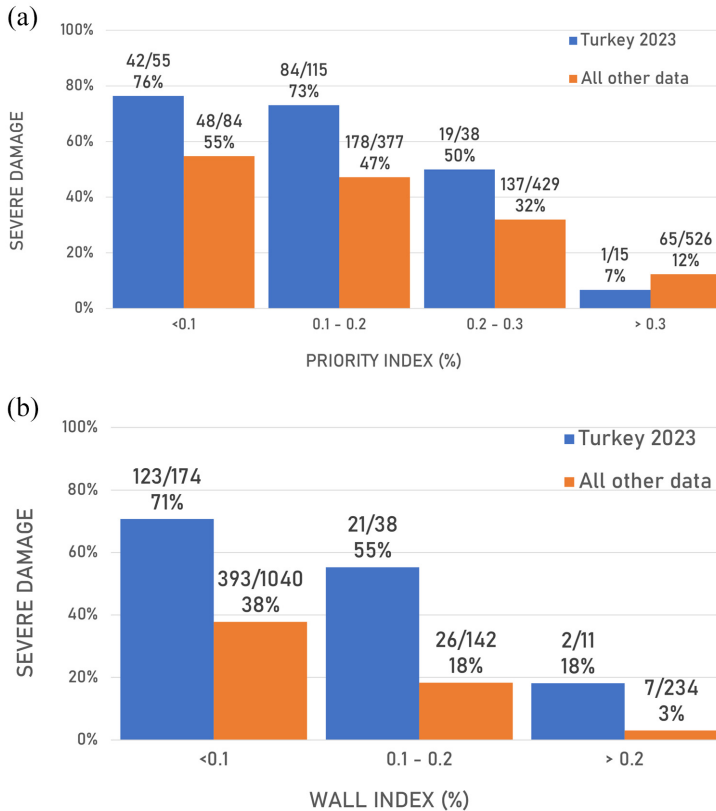


Figure 12. Percentage of surveyed buildings that were severely damaged versus (a) priority index and (b) wall index for the Turkey 2023 Earthquake and the combined data set.

average, less robust than other surveyed buildings according to the metrics proposed by Shiga et al. (1968), and Hassan and Sozen (1997).

Figure 13a shows the percentage of surveyed buildings classified as having severe damage after each considered event (Table 4) versus the average PI . Despite the chaotic nature and the complexity of the earthquake problem, Figure 13a can be used to suggest a general trend going from the upper left corner (large % of buildings having severe damage and small PI) down to the bottom right of the plot (low % of severely damaged buildings and large PI). The results reinforce the idea that as PI increases, the frequency of severe damage decreases despite the large number of relevant factors not included in the plotted data. The scatter in Figure 13a is related to differences in ground-motion intensity. For two sites with a similar average PI , the site with more intense shaking is likely to experience more damage. Consider the numbers for Turkey 2023 ($PGV \sim 90\text{cm/s}$), Christchurch 2011 ($PGV \sim 65\text{cm/s}$), and Mexico ($PGV \sim 30\text{cm/s}$). All three regions had similar average values of PI and WI ; however, the frequency of severe damage was greater in Turkey. Similarly, the 2017 China, and 1985; Mexico, 2008 Chile Earthquakes all had recorded PGV of 30 – 35 cm/s and there is a fairly linear reduction in the frequency of severe damage as average PI increased for these cases. Because of the large range in ground-motion intensity for the various survey sites, with PGV ranging from 30 to 90 cm/s , Figure 13b

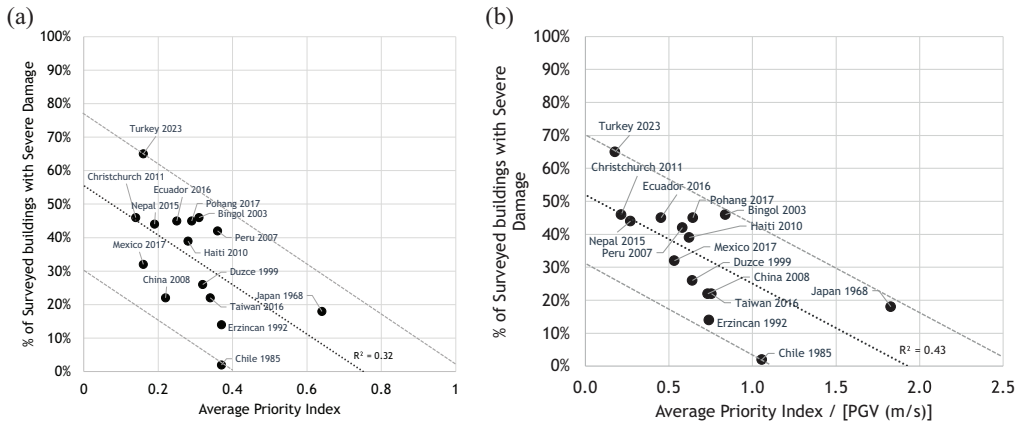


Figure 13: (a) Average priority index (%) and (b) average priority index (%) divided by peak ground velocity versus the percentage of severely damaged buildings for each earthquake event.

was plotted to assess the relationship between severe damage and the ratio of average *PI* to average *PGV* (Table 4). Figure 13b suggests a slightly clearer trend than Figure 13a does.

Figure 14 compares the values of *WI* across all the events in Table 4. The figure shows radical disparities relative to the indices observed in Japan and Chile. For reference, consider again that the guidelines published by ACI 314R-16 (2016) include an implicit limit for *WI* of 0.2%. Figure 14 does not show a clear trend to increase building robustness in Turkey since 1992. Because previous surveys in Turkey focused on buildings with 7 or fewer stories, consider for reference that the average values of *PI* and *WI* obtained for buildings of similar height in 2023 are 0.2 and 0.08 (in contrast with 0.17 and 0.07 obtained for the entire sample from 2023). No clear changes in robustness were observed either among buildings built before and after 2018, when the last regulation update was implemented in Turkey.

Drift control versus detailing

The two 13-story buildings in Figure 15 were in Antakya. They were reported to have been built by the same contractor following the same set of drawings. The detailing observed was one of the best in that (1) crossies were present, (2) tie spacing seemed uniform and acceptable, and (3) splices had enough confinement and cover to develop the strength of and reach fracture in longitudinal bars (Figure 15b). A permanent drift ratio of 6% was measured in the first story of the standing building. For an assumed value of $PGV = 1.3m/s$ (consistent with the most demanding spectrum in Figure 1), and $T = 1.3$ s, the roof drift can be estimated to have been $PGV \times T = 1.3 \times 1.3 = 1.7m$ (Puranam et al., 2019). For an approximate height of 39 m, roof drift ratio would be $1.7/39 = 4.3\%$, consistent with the observed permanent drift considering that the story drift ratio can be as high as 1.3 to 1.5 times the roof drift ratio.

These drift estimates are large enough to suspect overturning caused by second-order (p-delta) effects. The example illustrates the need to control drift to avoid collapse even if detailing is sufficient to produce a ductile response. The standing structure in Figure 15

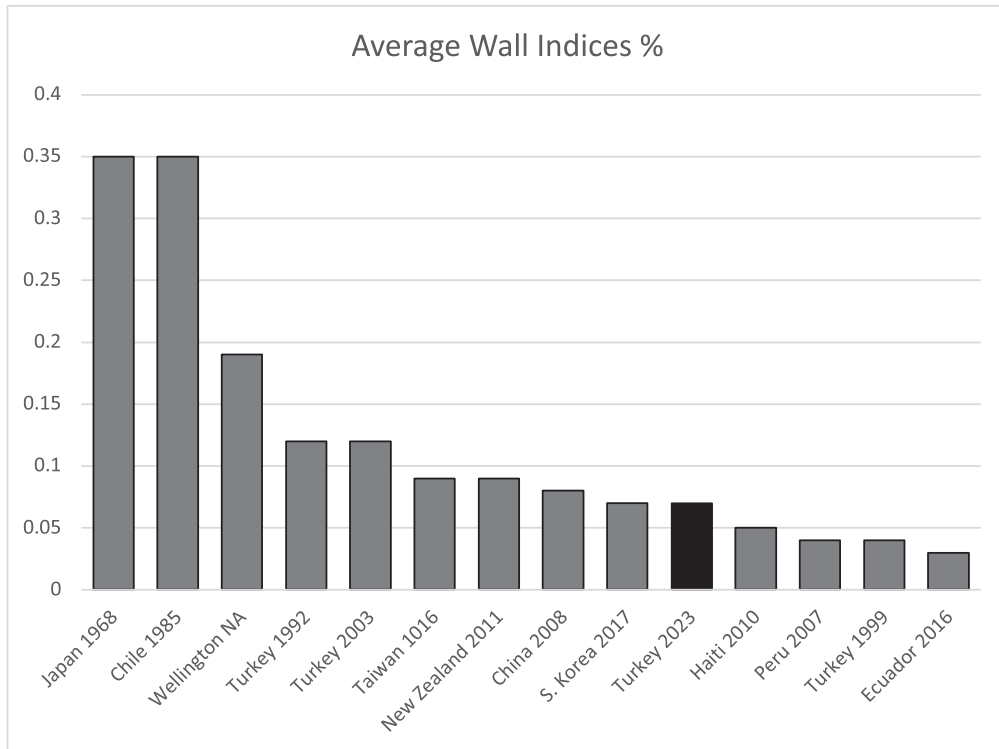


Figure 14. Comparison of average values of wall index from Turkey 2023, and with other events.

had $WI=0.04\%$ and $PI=0.11\%$. The wall and column densities were 0.5% and 0.8% , respectively.

This example and the previous section suggest strongly that to control damage, in Turkey and elsewhere, it is necessary to decrease drift demand through design limits leading to more robust structures. Detailing is necessary (to ensure stable hysteretic response) but not sufficient (to control damage).

Conclusion

The evidence collected supports the following conclusions:

1. Drift control must be the primary design objective in seismic regions, while maintaining ductility as a safeguard in the face of ground-motion uncertainty. Structures designed for earthquake resistance should possess both the necessary stiffness to limit drift and ensure functionality, as well as adequate drift capacity to prevent collapse during unforeseen events.
2. WI and CI (ratios of cross-sectional areas to total floor areas, WI and CI , as defined by Hassan and Sozen, 1997), correlated well with frequency of damage, with more than 90% of surveyed structures with $CI + WI < 0.1\%$ having severe damage (as defined here).



Figure 15. Building complex in Antakya: (a) building complex still standing with an approximate residual drift of 6% in the first story, and (b) identical structure that had collapsed (seen in the foreground of Figure 15a)

3. Approximately 96% of structures with critical damage (i.e. structures in a precarious state and judged to have been compromised to survive an aftershock) had $WI < 0.1\%$.
4. Engineers and contractors in Turkey and other regions facing similar seismic risk should be compelled to produce buildings with $CI + WI > 0.25\%$ or, at the very least, $WI > 0.2\%$ as implied by ACI 314R-16 (2016) guidelines.
5. Hassan and Sozen's initial proposal favored using the CI and WI for retrofit resource prioritization, but current observations support their use in crafting design criteria for more resilient structures, especially emphasizing the WI index as a design threshold within specified parameters.
6. Dividing WI and CI by intensity measures (e.g. S_d) produced modest improvements in correlations between damage frequency and $CI + WI$.
7. Regardless of building height, wall and column densities (ratios of sums of wall cross-sectional areas and column areas to typical floor plan) did not help organize the data from severely damaged buildings better than WI and CI (ratios of cross-sectional areas to total floor plan area).
8. PGV and S_d correlated better than other intensity measures with the percentage of damaged buildings.
9. Frame structures with shallow beams were observed to have been more vulnerable than comparable structures with regular beams (deeper than the supported floors).
10. Structural-wall buildings with walls uniformly distributed in both principal floor plan directions performed well.

11. There were numerous detailing problems revealed by the excessive drift that was induced by high intensities (associated with values of PGV of 100 cm = s or more) including:
 - lack of ties in plastic hinges;
 - lack of ties in beam-column joints;
 - lack of ties in column-grade-beam joints;
 - discontinuous bars in beams;
 - lack of stirrups in beams;
 - lack of crossties and hoops in walls; and
 - short and not-well-confined lap splices near critical sections of structural walls and columns.
12. To allow large drift and depend nearly exclusively on detailing (ductility) to control damage did not pay off. Had the detailing worked, the drift would have still been too large. There were observations of permanent drift ratios as high as 6%.
13. New, less brittle, or isolated partitions restrained out-of-plane are needed for buildings close to active faults.
14. Given the intensity of the ground motion, the damage observed in Turkey in 2023 is:
 - consistent with damage observed in Turkey before,
 - consistent with damage observed elsewhere, and
 - at least in part, the result of international design practices allowing the construction of buildings without the robustness necessary to control drift effectively.


Declaration of conflicting interests


The author(s) declared no potential conflicts of interest with respect to the research, authorship, and/or publication of this article.

Funding

The author(s) disclosed receipt of the following financial support for the research, authorship, and/or publication of this article: This research was funded by ACI, with additional support from American Society of Civil Engineers, and the US National Institute for Standards and Technology. The help of all other participating institutions and individuals is also gratefully acknowledged (M. Fırat Aydın, Bashar Abdo, Rebecca H. Collins, Fatih Canakci, Gurhan Comlekoglu, Mert Demir, Korhan Dalgic, Oscar Forero, Atakan Gokturk, Uveys Gozun, M. Fethi Gullu, Polat Gulkan, Ekin Gultepe, Amin Hariri, Ayhan Irfanoglu, Lissette Iturburu, Mehmet Enes Kaya, Mursel Kayıkcı, Edagul Kirpik, Kerim Kurt, Marko Marinkovic, Bora Ozkan, Mario Rodriguez, Julian Rincon, Cem Ali Sagır, Matthew Speicher, Bahaa Tayba, Koray Tureyen, Cennet Yesilyurt, and Reid Zimmerman for their help in data collection, Kahramanmaraş Dulkadiroğlu, and Türkoğlu Municipalities Urban Planning Departments, İbrahim Köroğlu from Kahramanmaraş İstiklal University Department of Construction for providing access to the structural drawings of some buildings investigated, and İzmir Institute of Technology for the administrative support in getting the necessary permits to access the earthquake-affected cities.

ORCID iDs

Santiago Pujol  <https://orcid.org/0000-0002-9888-1867>

Meltem Eryilmaz-Yildirim  <https://orcid.org/0000-0003-2750-0235>

Baki Ozturk  <https://orcid.org/0000-0002-2319-0447>

Supplemental material

Supplemental material for this article is available online.

References

- AFAD (2023) Republic of Turkey, Ministry Of Interior Disaster And Emergency Management Presidency, department of earthquake, Turkish accelerometric database and analysis system. Available at: <https://tadas.afad.gov.tr/> (accessed 8 July 2023).
- Alcocer S, Behrouzi A, Brena S, Elwood KJ, Irfanoglu A, Kreger M, Lequesne R, Mosqueda G, Pujol S, Puranam A, Rodriguez M, Shah P, Stavridis A and Wood R (2020) Observations about the seismic response of RC buildings in Mexico City. *Earthquake Spectra* 36(Suppl. 2): 154–174.
- American Concrete Institute (ACI) (2016) *Guide to Simplified Design for Reinforced Concrete Buildings, ACI 314R-16*. Farmington Hills, MI: ACI.
- American Concrete Institute (ACI) (2019) *Building Code Requirements for Structural Concrete and Commentary, ACI 318-19*. Farmington Hills, MI: ACI.
- American Concrete Institute (ACI) (2023) *ACI 133 Building Inspection Recommendations*. Farmington Hills, MI: ACI.
- Cuadra C, Saito T and Zavala C (2013) Diagnosis for seismic vulnerability evaluation of historical buildings in Lima, Peru. *Journal of Disaster Research* 8(2): 320–327.
- Dönmez C (2015) Seismic performance of wide-beam infill-joist block RC frames in Turkey. *Journal of Performance of Constructed Facilities* 29(1): 04014026.
- Fintel M (1991) Shearwalls-An answer for seismic resistance? *Concrete International* 13(7): 48–53.
- García LE, Perez A and Bonacci J (1996) Cost implications of drift controlled design of reinforced concrete buildings. In: *11th world conference on earthquake engineering*, Acapulco, Mexico, 23–28 June.
- Gemici B (2019) *Investigation of the effect of structural grid discontinuity on the earthquake behavior of midrise RC moment frames*. Master of Science Thesis. Izmir Institute of Technology (IYTE), Izmir, Turkey.
- Gur T, Pay A, Ramirez JA, Sozen MA, Johnson AM, Irfanoglu A and Bobet A (2009) Performance of school buildings in Turkey during the 1999 Düzce and the 2003 Bingöl earthquakes. *Earthquake Spectra* 25(2): 239–256.
- Hassan F and Sozen MA (1997) Seismic vulnerability assessment of low-rise buildings in regions with infrequent earthquakes. *ACI Structural Journal* 94(1): 31–39.
- Howe GE (1936) Requirements for buildings to resist earthquakes. *American Institute of Steel Construction*.
- O'Brien P, Eberhard M, Haraldsson O, Irfanoglu A, Lattanzi D, Lauer S and Pujol S (2011) Measures of the seismic vulnerability of reinforced concrete buildings in Haiti. *Earthquake Spectra* 27(Suppl. 1): 373–386.
- Pledger L, Pujol S and Chandramohan R (2023) Investigating the effect of stiffness on the seismic performance of RC structures. In: *2023 NZSEE annual conference*, Auckland, New Zealand, 19–21 April.
- Pujol S, Irfanoglu A and Puranam A (2022) *Drift-Driven Design of Buildings: Mete Sozen's Works on Earthquake Engineering*. Boca Raton, FL: CRC Press.
- Pujol S, Laughery L, Puranam A, Hesam P, Cheng LH, Lund A and Irfanoglu A (2020) Evaluation of seismic vulnerability indices for low-rise reinforced concrete buildings including data from the 6 February 2016 Taiwan earthquake. *Journal of Disaster Research* 15(1): 9–19.
- Puranam AY, Irfanoglu A, Pujol S, Chiou TC and Hwang SJ (2019) Evaluation of seismic vulnerability screening indices using data from the Taiwan earthquake of 6 February 2016. *Bulletin of Earthquake Engineering* 17(4): 1963–1981.
- Riddell R, Wood SL and de la Llera JC (1987) *The 1985 Chile earthquake: Structural characteristics and damage statistics for the building inventory in Vina del Mar*. Civil Engineering Studies SRS-534. Urbana, IL: University of Illinois Engineering Experiment Station. College of Engineering

- University of Illinois at Urbana-Champaign. Available at: <https://hdl.handle.net/2142/14160> (accessed 8 July 2023).
- Shah PP (2021) *Seismic drift demands*. PhD Dissertation. Purdue University, West Lafayette, IN.
- Shah PP, Pujol S, Kreger M and Irfanoglu A (2017) 2015 Nepal earthquake damage assessment survey. *Concrete International* 39(3): 42–49.
- Shiga T, Shibata A and Takahashi T (1968) Earthquake Damage and Wall Index of Reinforced Concrete Buildings. Proc. Tohoku District Symposium, *Architectural Institute of Japan*, No. 12, Dec., 29–32 (in Japanese).
- Shiga T (1997) Earthquake damage and the amount of walls in reinforced concrete buildings. In: *World Conference Earthquake Engineering*, 6 (pp. 2467–72).
- Sim C, Song C, Skok N, Irfanoglu SA, Pujol S and Sozen M (2015) Database of low-rise reinforced concrete buildings with earthquake damage. Available at: <https://datacenterhub.org/resources/> (accessed 8 July 2023).
- Sozen MA (1980) Review of earthquake response of reinforced concrete buildings with a view to drift control. In: *7th world conference on earthquake engineering*, Istanbul, Turkey.
- T.C. Bayındırlık Bakanlığı (Turkish Ministry of Public Works) (1940) *Zelzele Mıntıklarında Yapılacak Insaatlara Ait İtalyan Yapı Talimatnamesi (Italian Building Code for the Construction in the Earthquake Zones) (ZMYİAİYT-1940)*.
- US Geological Survey (USGS) (2023a) Earthquake data web page for the 6 February 2023 magnitude 7.5 Elbistan earthquake, Kahramanmaraş earthquake sequence in Turkey. Available at: <https://earthquake.usgs.gov/earthquakes/eventpage/us6000jlqa/executive> (accessed 8 July 2023).
- US Geological Survey (USGS) (2023b) Earthquake data web page for the 6 February 2023 magnitude 7.8 Pazarcik earthquake, Kahramanmaraş earthquake sequence in Turkey. Available at: <https://earthquake.usgs.gov/earthquakes/eventpage/us6000jllz/executive> (accessed 8 July 2023).
- Villalobos E, Sim C, Smith-Pardo JP, Rojas P, Pujol S and Kreger ME (2018) The 16 April 2016 Ecuador earthquake damage assessment survey. *Earthquake Spectra* 34(3): 1201–1217.
- Wald DJ, Quitoriano V, Heaton TH and Kanamori H (1999) Relationships between peak ground acceleration, peak ground velocity, and modified Mercalli intensity in California. *Earthquake Spectra* 15(3): 557–564.
- Zhou W, Zheng W and Pujol S (2013) Seismic vulnerability of reinforced concrete structures affected by the 2008 Wenchuan earthquake. *Bulletin of Earthquake Engineering* 11(6): 2079–2104.